IJASRM
International Journal of Advanced Scientific Research and Management, Volume 3 Issue 12, Dec 2018
www.ijasrm.com
ISSN 2455-6378

Removal of anionic dye Congo red from aqueous solution by ZnO-Montmorillonite as adsorbent: Equilibrium and kinetics

P. Gowtham[1], B. Kavitha[2*], R. Arunadevi[3], R. Sivaperumal[4*]

[1,4*] Department of Chemistry, Theni College of Arts and Science, Veerapandi, Tamilnadu—625534, India

[2*,3] P.G and Research Department of Chemistry, Cardamom Planter's Association college, Bodinayakanur, Tamilnadu-625513, India

Abstract

The adsorption efficiency of ZnO-Montmorillonite (ZnO-MMT) nanoparticles was evaluated by the removal of Congo red. The results showed that the adsorption of Congo red on ZnO-Montmorillonite was much higher than that of pure ZnO. X-ray diffraction analysis confirms the formation of pure wurtzite ZnO phase with crystallite size in the 11-19 nm range, while scanning electron microscopic observation revealed agglomerated spherical morphology of ZnO-MMT. The band gap of the as-prepared NPs calculated on the basis of Tauc approach and it was found to be lower than the known band gap energy of bulk ZnO (3.37 eV).

Keywords: *ZnO, Montmorillonite, photocatalytic activity, wurtzite*

1. Introduction

The major sources of pollution in water and air are chemicals released from industries. Textile industry is one of the major sources of the pollutants such as coloured organic reagents; the dyes. The presence of such pollutants in ground and surface water are harmful to human as well as aquatic life. Some of them are carcinogenic and mutagenic as well as genotoxic and therefore, a technology for cleaning the water is very important [Robinson, McMullan, 2001]. Therefore, it is necessary to find innovative and cost-effective methods for the safe and complete destruction of these organic compounds Conventional methods for removing dissolved heavy metal ions include chemical precipitation, chemical oxidation and reduction, ion exchange, filtration, electrochemical treatment and evaporative recovery. However, these high technology processes have significant disadvantages, including incomplete metal removal, requirements for expensive equipment and monitoring systems, high reagent or energy requirements or generation of toxic sludge or other waste products that require disposal. Zinc oxide (ZnO) is one of the most important II-VI semiconductors because of its interesting and unique characteristics, including wide band gap (3.37 eV), large exciton binding energy (60 meV), physical and chemical stability, biocompatibility, nontoxicity, high photosensitivity, piezoelectric and pyroelectric properties
[Wang, Xie, 2009, Umar, Chauhan, 2011, Ghorbel-Abid, Galai, 2010, Chakir, Bessiere, 2002, Coetzee, Puka, 2003, Ayari, Srasra, 2007, Ayari, Srasra, 2007, Ramesh, Leea, 2007, Barbier, Duc, 2000].

Clays have been evaluated for their purifying qualities since they are thought to act as a filter and purifier of pollutants**.** Given their high impermeability, clays are often used as pollution barrier for waste storage sites. Kumric et al. [Kumrić, Đukić, 2013] have reported that mechanochemically treated interstratified montmorillonite/kaolinite clay showed considerably improved sorption ability with regard to the raw clay. This was attributed to the microstructural changes induced by milling for different periods of time (1, 2, 10 and 19 h). Improvement of the sorption ability of the clay with milling was explained by the increase of the surface available for adsorption due to exfoliation of clay particles and decrease of clay particle size. Montmorillonite has been traditionally applied regarding the removal of metalions and organic contaminants from drinking and waste water. The adsorption properties of montmorillonite can often been chanced either by the intercalation of metal ions in the space between the layers. Of these modifications,clays with metal ions inter layered have been broadly analyzed recently [Aouad, Mandalia, 2005].

In the present paper, a simple and inexpensive method is proposed to synthesize the ZnO-Montmorillonite NPs at low temperature using a co-

IJASRM International Journal of Advanced Scientific Research and Management, Volume 3 Issue 12, Dec 2018
www.ijasrm.com
ISSN 2455-6378

precipitation approach without the use of template or surfactant. The effects of various operational parameters, such as initial dye concentration, initial pH and adsorbent dosage on the removal of Cango red are also investigated. The adsorption kinetic and isothermal properties were also investigated.

2. Experimental section

2.1 Materials

Zinc acetate, Distilled water, Sodium hydroxide, Montmoritrollite was purchased from Merck specialities Private limited. All reagents were used as received without further purification. Deionized water was used in all experiments.

2.2. Preparation of Zinc oxide Nanoparticle

Zinc oxide nanostructures were prepared by co-precipitation method. 90 ml of 0.02M zinc acetate was added, after addition of 10ml of above prepared milky latex, 2.0 M NaOH aqueous solution was introduced into the above aqueous solution, resulting in a white aqueous solution at pH 8, which were then placed on magnetic stirring for 2 hr. The precipitate was then taken out and washed repeatedly with distilled water followed by ethanol to remove the impurities for the final products. Then a white powder was obtained after drying at 60^0 C in hot air oven for 3hr.

2.3. Preparation of Zinc oxide/MMT Nanoparticle

The ZnO/MMT nanoparticles were prepared using chemical co-precipitation technique. 2.0 g of montmorillonite and 90 ml of 0.02M zinc acetate was added, after addition of 10ml of above prepared milky latex, 2.0 M NaOH aqueous solution was introduced into the above aqueous solution, resulting in a white aqueous solution at pH 8, which were then placed on magnetic stirring for 2 hr Finally, the suspensions were centrifuged, washed twice with distilled water and ethanol, and kept for 2 h in a muffle furnace at 100 °C.

2.4. Adsorbate

The Congo red dye was first synthesized in 1883 by Paul Bottiger who was working then for the Friedrich Bayer Company in Elberfeld, Germany. Due to a color change from blue to red at pH 3.0-5.2, Congo red can be used as a pH indicator. It is the sodium salt of benzidinediazo-bis-1-naphthylamine-4-sulfonic acid (formula: $C_{32}H_{22}N_6Na_2O_6S_2$; molecular weight: 696.66 g/mol). It is a secondary diazo dye. λ_{max} = 497nm

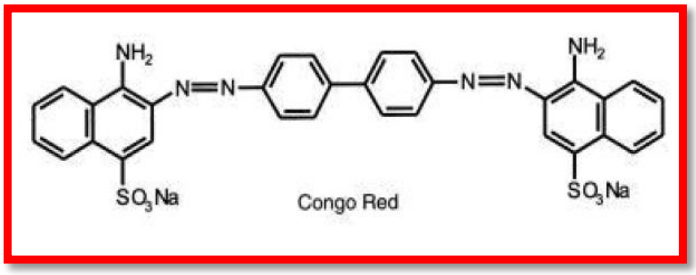

Fig. 1. Structure of Congo red

2.5. Adsorption experiments

Batch-mode adsorption studies were carried out by adding 2.0 mg adsorbent and 5 µM dye solution of certain concentration in colorimeter tubes. After desired adsorption time, a suitable amount of supernatant was drawn by the aid of a magnet to attract the adsorbent. Then, the supernatant was analyzed using a TU-1901 double beams UV–vis spectrophotometer (China) at -max = 526.00 nm. The adsorption capacity of the adsorbent was calculated by Eq. (1):

$$q_t = \frac{1000(C_0 - C_t)VM_r}{W} \quad \textbf{(1)}$$

where C_0 (mol L^{-1}) is the initial CR concentration, C_t (mol L^{-1}) is CR concentration in supernatant at time t (min) obtained through calibration curve, V (L) is volume of the sample solution, M_r is the molar mass of CR, and W (g) is the weight of adsorbent.

2.6. Characterization techniques

The synthesized nanocomposite was characterized by the following methods. The UV-vis diffuse reflection spectra were obtained for the dry-pressed disk samples using a JASCO V-550 double beam spectrophotometer with PMT detector equipped with an integrating sphere assembly, using $BaSO_4$ as a reference sample. The spectra were recorded at room temperature ranging from 200nm to 800nm. The crystal phase and composition of the nanocomposite was analysed using X-ray powder diffraction with Cu Kα radiation 25^oC using XPERT PRO X-RAY and the structural assignments were made with reference to the standard JCPDS powder diffraction files. Scanning electron microscopy (SEM) observations were performed by means of a JSM 6701F-6701 instrument in both secondary and backscattered electron modes. The elemental analysis was detected by an energy dispersive X-ray spectroscopy (EDX) attached to the SEM.

3. Results and Discussion

3.1. UV-vis-DRS

The band gaps were calculated using Tauc

IJASRM
International Journal of Advanced Scientific Research and Management, Volume 3 Issue 12, Dec 2018
www.ijasrm.com
ISSN 2455-6378

equation:

$$1.\ (\alpha h\upsilon)^{1/2} = A(h\upsilon - E_g) \quad (2)$$

Where α is the absorbance, hν is the incident photon energy, and A is a constant. The band gaps (E_g) were determined from extrapolation of linear fit onto the X-axis. The band gaps of ZnO-MMT was found to be 2.5 eV respectively. The band gap values are nearer to the generally accepted value for bare ZnO. Generally, the highest adsorption efficiency is due to the narrow band gap.

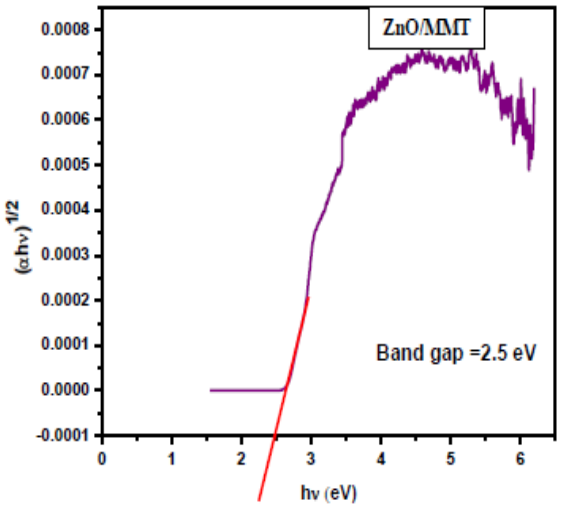

Fig. 2. Band gap of ZnO/MMT

3.2. XRD

The XRD profiles of ZnO and ZnO-*Montmorillonite* are shown in Fig. 3. The diffraction peaks of ZnO-*Montmorillonite* at 2θ of 25.24, 37.86, 48.05, 53.89, 54.97, 62.62, 68.69, 70.39 and 75.13 are consistent with those of wurtzite phase ZnO (JCPDS-36-1451) and no impurity peaks appeared. The peak intensities are slightly reduced when compared to that of ZnO. The average crystallite size was measured on the basis Debye-Scherer equation [Arunadevi, Kavitha, 2017]. The average crystallite size of ZnO and ZnO-*Montmorillonite* is found to be 19.6 9 nm and 11.47 nm respectively. There is a slight decrease in the crystallite size of ZnO after surface modification with *Montmorillonite*.

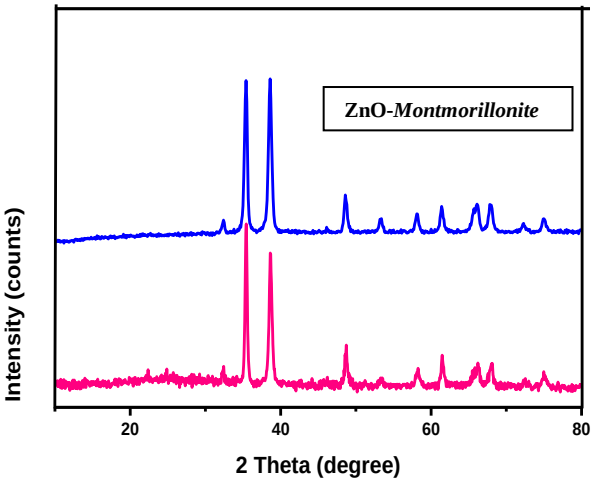

Fig. 3. XRD of ZnO and ZnO-Montmorillonite

3.3. SEM and EDX

The synthesized nanoparticles are examined for the information regarding their physical feature using a SEM. Fig.4 shows the SEM image of ZnO-Montmorillonite nanoparticles. It confirmed that the Montmorillonite act as a surface modifier and have a better dispersity. When Montmorillonite is doped on the surface modified ZnO with plant extract revealed to be well crystallized and also slightly agglomerated spherical nanoparticles. It can form more number of activities sites, consecutively photocatalytic activity also increases.

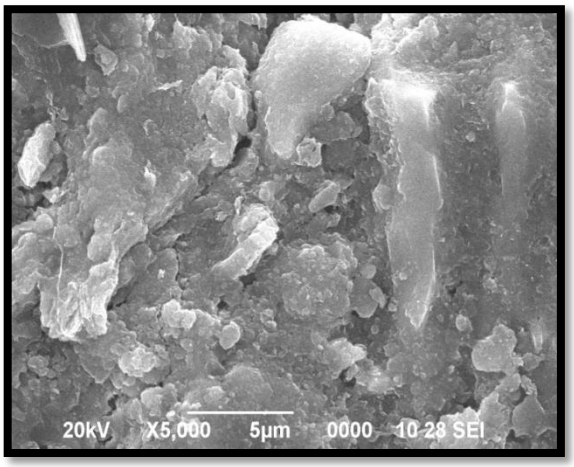

Fig. 4. SEM image of ZnO-Montmorillonite

IJASRM
International Journal of Advanced Scientific Research and Management, Volume 3 Issue 12, Dec 2018
www.ijasrm.com
ISSN 2455-6378

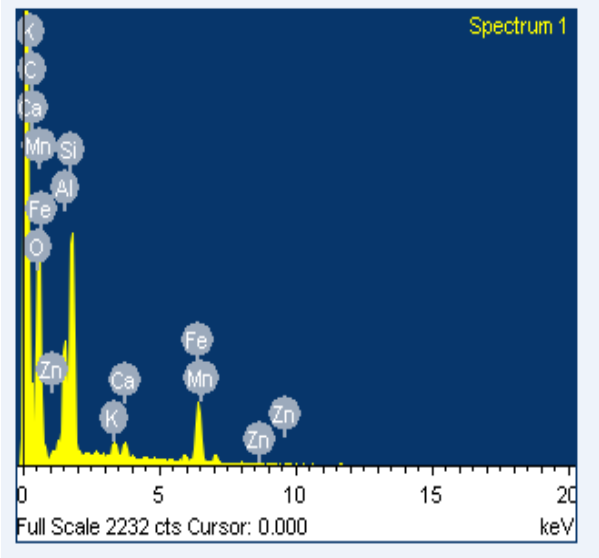

Fig. 5. EDX spectrum of ZnO-Montmorillonite

3.4. Effect of initial dye concentration

The adsorption capacity is dependent on the initial dye ion concentration. The dependence of adsorption capacity of ZnO nanoparticles on initial concentration of dye was (5 µM to 20 µM) shown in Fig. 6. As seen from Fig. 6, equilibrium uptake has been increased with increase in the initial dye concentration in the range of concentrations studied. The increase in adsorption capacity with an increase in initial dye concentration is a result of the increase in driving force due to concentration gradient developed between the bulk solution and surface of the nanoparticles. At higher concentration of dye, the active sites of ZnO nanoparticles were surrounded by much more dye and the process of adsorption continues, leading to an increased uptake of metal ions from the solution. Therefore, the values of qe increased with the increase of initial dye concentrations (C_0).

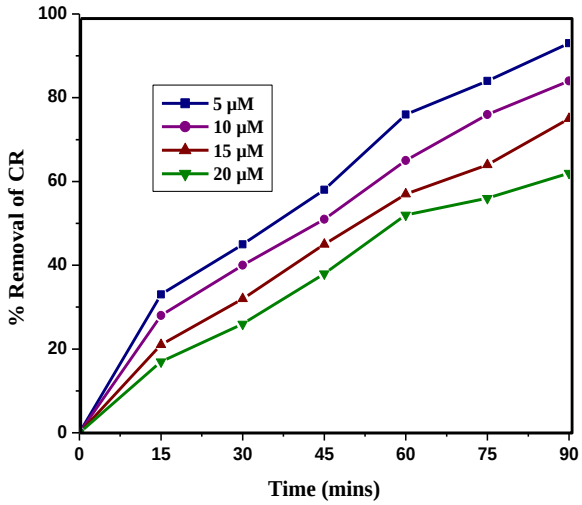

Fig. 6. Effect of initial dye concentration

3.5. Influence of initial adsorbent dosage on dye removal

The amount of adsorbent dosage was varied in the given range 0.5 g, 1.0 g, 1.5 g, and 2.0 g. It was observed from the graphs that increasing the dosage increases the % removal of CR. As there was no drastic increase in the adsorption rate on increasing the dosage of adsorbent beyond 1.5 g of ZnO-*Montmorillonite*, hence, from economic point of view, 2.0 g was taken as optimum dosage for removal of CR. It can be attributed to the increase in adsorbent sites for more adsorption of the dye at the fixed 5 µM.

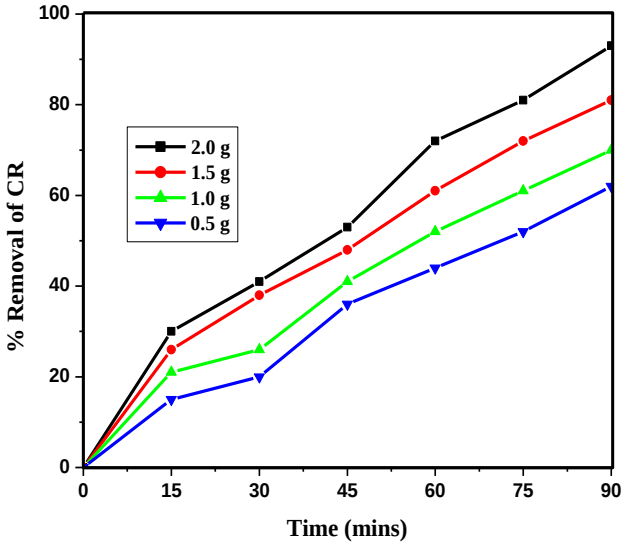

Fig. 7. Effect of adsorbent dose

3.6. Effect of initial pH of the solution

The effects of initial pH on dye solution of three dyes removal were investigated by varying the pH from 2 to 10. At pH - 2 the removal was minimum but it increased along with increasing initial pH of dye solution. For Congo red there is no significant change in amount adsorbed after pH 7. In fact adsorption found to decrease with increase in pH of solution. The adsorption of these positively charged dye groups on the adsorbent surface is primarily influenced by the surface charge on the adsorbent which in turn is influenced by the solution pH. The result showed that availability of negatively charged groups at the adsorbent surface is necessary for the adsorption of basic dyes to proceed which we see at pH -2 is almost unlikely as there is a net positive charge in the adsorption system due to the presence of H_3O^+ .Thus as the pH increased, more negatively charged surface was available thus facilitating greater dye removal .We see that the trend is increasing with increasing pH.

IJASRM
International Journal of Advanced Scientific Research and Management, Volume 3 Issue 12, Dec 2018
www.ijasrm.com
ISSN 2455-6378

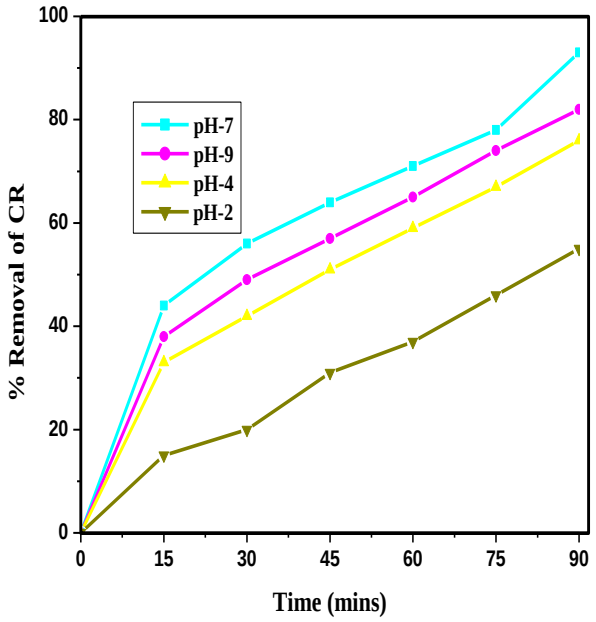

Fig. 8. Effect of pH

3.7. Adsorption of CR dye by ZnO

3.7.1. Adsorption isotherms

Equilibrium adsorption isotherm is the most important design parameter that describes how the adsorbate interacts with the adsorbent. By determining the adsorption capacity of an adsorbent and modeling of isotherms by different equilibrium models, an insight into both the sorption mechanism and affinity of the adsorbent could be elucidated. The Langmuir isotherm is derived assuming a uniform surface with finite identical sites and monolayer adsorption of the adsorbate [Gokhale, Jyoti, 2008]. The Langmuir isotherm is given by the relation (3):

$$q_e = \frac{q_m K_L C_e}{1 + K_L C_e} \qquad (3)$$

Where q_m is the maximum monolayer biosorption (mg g^{-1}) and k_L is the Langmuir constant (L mg^{-1}). Another essential characteristic of the Langmuir isotherm can be expressed by the separation factor or equilibrium factor (R_L) [Piccin, Vieira, 2009], as follows (4):

$$R_L = \frac{1}{1 + K_L C_0} \qquad (4)$$

The Freundlich adsorption isotherm gives the empirical relation between q_e and C_e [Gokhale, Jyoti, 2009]. The Freundlich isotherm is given by the relation (5):

$$q_e = K_F C_e^{1/n} \qquad (5)$$

where k_F is the Freundlich constant ((mg g^{-1})(mg L^{-1})$^{-1/n}$) and 1/n is the heterogeneity factor. Values of isotherm model parameters are summarized in Table 1. The adsorption process can be better fitted with the Freundlich isotherm model ($R^2 > 0.989$), which indicated the homogeneous distribution of active sites on the surface of ZnO/MMT NPs. The R_L values for Congo red were calculated and plotted against the initial dye concentration. Fig. 9 shows that, the sorption of congo red on ZnO/MMT increased as the initial dye concentration increased from 5 to 20 mg/L, indicating that adsorption is even favorable for the higher dye concentrations that have been investigated.

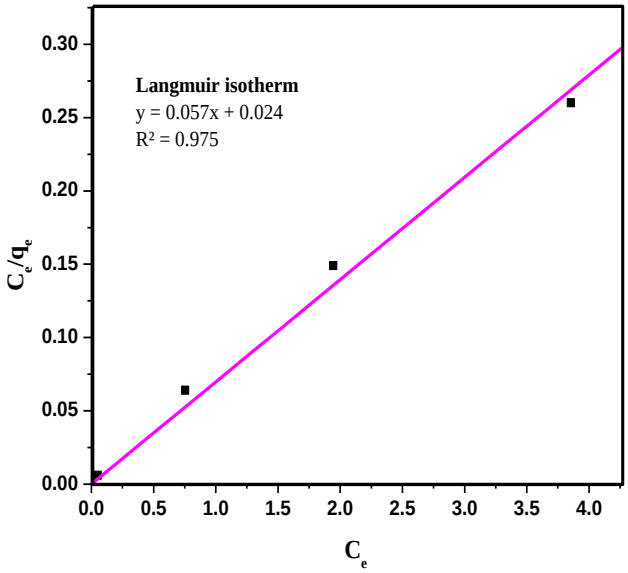

Fig. 9. Langmuir isotherm

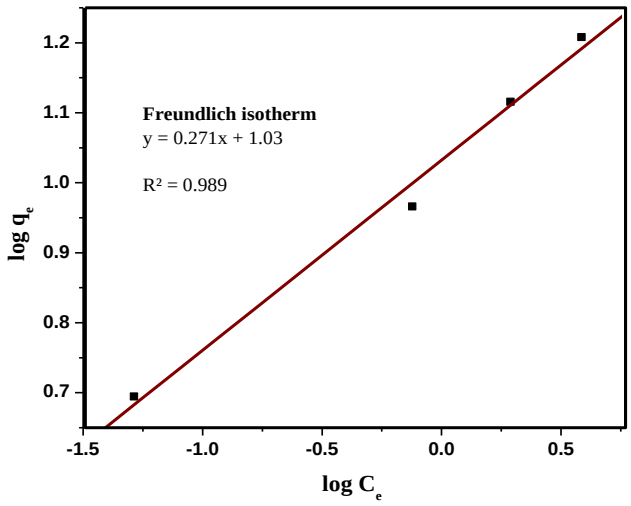

Fig. 10. Freundlich isotherm

3.7.2. Evaluation of adsorption kinetics

In order to predict the mechanism of the present adsorption process and evaluate the performance of the adsorbent, three well known kinetic models were used to fit the experimental data: pseudo-first-order, pseudo-second-order and

IJASRM
International Journal of Advanced Scientific Research and Management, Volume 3 Issue 12, Dec 2018
www.ijasrm.com
ISSN 2455-6378

intraparticle diffusion model. The pseudo-first-order kinetic model was described by Lagergren [Lagergren, Kung. Sven, 1898] and might be represented by Eq. (6):

$$\log(q_e - q_t) = \log q_e - \frac{k_1 t}{2.303} \quad \textbf{(6)}$$

Where q_e (mg g−1) and q_t (mg g−1) are the adsorption capacity at equilibrium and time t (min), respectively; k_1 (min−1) is the rate constant of pseudo-first-order kinetic model. Values of k_1 and q_e can be obtained from the slope and intercept of the plots of $\log(q_e - q_t)$ versus t (Fig. 11) for Eq. (2). The linear form of pseudo-second-order kinetic model was expressed by Eq. (7) [Ho, McKay,1998, Arunadevi, Kavitha, 2018].

]:

$$\frac{t}{q_t} = \frac{1}{k_2 q_e^2} + \frac{t}{q_e} \quad \textbf{(7)}$$

Where k_2 (g mg^{-1} min^{-1}) is the rate constant of pseudo-second order kinetic model. Values of qe and k_2 can be obtained from the linear plots of t/qt (Fig. 12) against t for Eq. (7). All the experimental data showed better agreement with pseudo-second-order model in terms of higher correlation coefficient value (R^2 > 0.988) and lower deviation between experimental and calculated qe values.

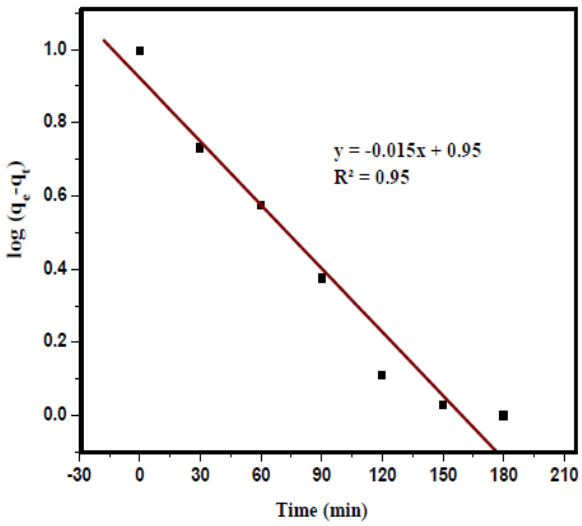

Fig. 11. Pseudo first order kinetic model

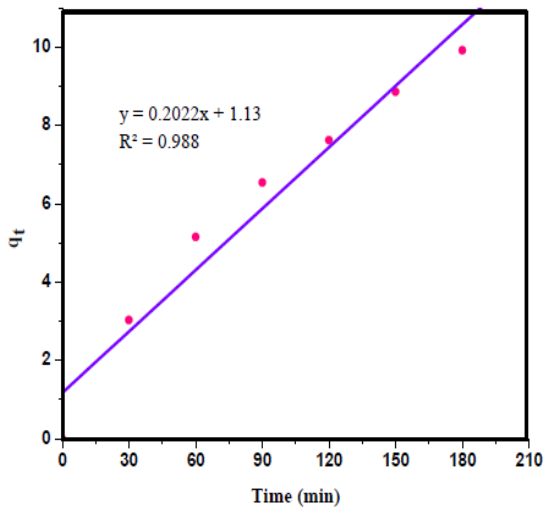

Fig. 12. Pseudo second order kinetic model

4. Conclusion

In this work, the use of the clay modified nanoparticles to solve the problem of dye loaded wastewater was addressed. The adsorption efficiency was influenced by various parameters such as initial dye concentration, dose of adsorbent and pH. The removal efficiency increased with decreasing dye concentration and increasing dose of adsorbent. The Langmuir and Freundlich adsorption isotherm models were used for the description of the adsorption equilibrium of CR dye onto ZnO-*Montmorillonite*. The data were in good agreement with the Freundlich isotherm rather than the Langmuir isotherm. Clay modified ZnO have been evaluated for their purifying qualities since they are thought to act as a filter and purifier for pollutants. Our results provide further support of this view reaffirming that certain clays could be a promising agent in the fight against organic pollutants in waste water when used as pollution barriers in waste storage sites.

References

[1] T. Robinson, G. McMullan, R. Marchant, P. Nigam, Bioresour. Technol. 77 (2001) 247–255.
[2] D. S. Wang, T. Xie, Y. D; Li, Nano Research. 2 (2009) 30-46.
[3] Umar, M.S. Chauhan, S. Chauhan, R. Kumar, G. Kumar, S.A. Al-Sayari, S.W. Hwang, A. Al-Hajry, J Colloid Interface Science. 363 (2011) 521–528.
[4] Ghorbel-Abid, A. Jrad, K. Nahdi, M. Trabelsi-Ayadi, Desalination 246 (2009) 595–604.
[5] Ghorbel-Abid, K. Galai, M. Trabelsi-Ayadi, Desalination 256 (2010) 190–195.
[6] Chakir, J. Bessiere, K. ElKacemi, B. Marouf, J Hazard Mater (2002) 29–46.
[7] L. L. Coetzee, R. Puka, S. Mubenga, Water SA 29 (2003) 331–338.
[8] F. Ayari, E. Srasra, M. Trabelsi-Ayadi, Desalination 206 (2007) a 270–272.
[9] F. Ayari, E. Srasra, M. Trabelsi-Ayadi, Desalination 206 (2007) b 499–506.
[10] Ramesh, D. J. Leea, J. W. C. Wong, J Colloid Interface Science 307 (2007) 531–554.
[11] F. Barbier, G. Duc, M. Petit-Ramel, Colloid Surface A 166 (2000) 153–159.
[12] K.R. Kumrić, A.B. Đukić, T.M.Trtić-Petrović, N.S.Vukelić, Z. Stojanović, J.D.Grbović Novaković, Lj.Matović, Ind.Eng.Chem.Res.52 (2013) 7930–7939.
[13] Aouad, T. Mandalia, F. Bergaya. Appl Clay Sci 28 (2005) 175–82.
[14] R. Arunadevi, B. Kavitha, P. Pandi Sudha, M. Rajarajan, A. Suganthi, Desalination and Water Treatment, 78 (2017) 330–340
[15] S. V. Gokhale, K. K. Jyoti, S. S. Lele, Bioresour. Technol. 99 (2008) 3600–3608.
[16] J. S. Piccin, M. L. G. Vieira, J. Gonçalves, G. L. Dotto, L. A. A. Pinto, J. Food Eng. 95 (2009) 16.
[17] S. V. Gokhale, K. K. Jyoti, S. S. Lele, J. Hazard. Mater. 170 (2009) 735–743.
[18] S. Lagergren, Kung. Sven. Veten. Hand. 24 (1898) 1–39.
[19] Y.S. Ho, G. McKay, Can. J. Chem. Eng. 76 (1998) 822–827.
[20] R. Arunadevi, B. Kavitha, Int.J.Trend. Sci.Research.Development. 2 (2018) 1775-1782.